Title
Structure of a human rhinovirus complexed with its receptor molecule.

Journal
Proceedings of the National Academy of Sciences of the United States of America, 90(2)

ISSN
0027-8424

Authors
Olson, NH
Kolatkar, PR
Oliveira, MA
et al.

Publication Date
1993

DOI
10.1073/pnas.90.2.507

Peer reviewed

Proc. Natl. Acad. Sci. USA
Vol. 90, pp. 507–511, January 1993
Biochemistry

Structure of a human rhinovirus complexed with its receptor molecule

NORMAN H. OLSON*, PRASANNA R. KOLATKAR*, MARCOS A. OLIVEIRA*, R. HOLLAND CHENG*, JEFFREY M. GREVE†, ALAN MCCLELLAND†‡, TIMOTHY S. BAKER*, AND MICHAEL G. ROSSMANN*§

*Department of Biological Sciences, Purdue University, West Lafayette, IN 47907-1392; and †Institute for Molecular Biologicals, Miles Inc., 400 Morgan Lane, West Haven, CT 06516-4175

Contributed by Michael G. Rossmann, October 7, 1992

ABSTRACT **Cryoelectron microscopy has been used to determine the structure of a virus when complexed with its glycoprotein cellular receptor. Human rhinovirus 16 complexed with the two amino-terminal, immunoglobulin-like domains of the intercellular adhesion molecule 1 shows that the intercellular adhesion molecule 1 binds into the 12-Å deep "canyon" on the viral surface. This result confirms the prediction that the viral–receptor attachment site lies in a cavity inaccessible to the host's antibodies. The atomic structures of human rhinovirus 14 and CD4, homologous to human rhinovirus 16 and intercellular adhesion molecule 1, showed excellent correspondence with observed density, thus establishing the virus–receptor interactions.**

Human rhinoviruses are one of the major causes of the common cold. They, like other picornaviruses, are icosahedral assemblies of 60 protomers that envelope a single, positive-sense strand of RNA. Each protomer consists of four polypeptides, VP1–VP4. The three external viral proteins (VP1–VP3) each have an approximate M_r of 30,000 and a similar folding topology (1, 2). The external viral radius is ≈150 Å, and the total molecular weight is roughly 8.5×10^6. A surface depression, or canyon, that is ≈12 Å deep and 12–15 Å wide, encircles each pentagonal vertex (Fig. 1*c*). Residues lining the canyon are more conserved than other surface residues among rhinovirus serotypes (5). The most variable surface residues are at the sites of attachment of neutralizing antibodies (1, 6, 7). It has been proposed that the cellular receptor molecule recognized by the virus binds to conserved residues in the canyon, thus escaping neutralization by host antibodies that are too big to penetrate into that region. This hypothesis (1, 8) is supported by site-directed mutagenesis of residues lining the canyon that alters the ability of the virus to attach to HeLa cell membranes (9). Also, conformational changes in the canyon floor, produced by certain antiviral agents that bind into a pocket beneath the canyon floor, inhibit viral attachment to cellular membranes (10). Conservation of the viral-attachment site inside a surface depression has been observed for Mengo (11) and influenza virus (12).

There are well over 100 human rhinovirus serotypes, which can be divided into roughly two groups according to the cellular receptor they recognize (13, 14). The structures of human rhinovirus 14 (HRV-14) (1), which belongs to the major group of serotypes, and of HRV-1A (15), which belongs to the minor group of serotypes, have been determined. There are at least 78 serotypes (16) that bind to intercellular adhesion molecule 1 (ICAM-1), the major group rhinovirus receptor (17, 18). The ICAM-1 molecule has five immunoglobulin-like domains (D1–D5, numbered sequentially from the amino end), a transmembrane portion, and a small cytoplasmic domain (19, 20). Domains D2, D3, and D4 are glycosylated. Unlike immunoglobulins, ICAM-1 appears to be monomeric (18). Mutational analysis of ICAM-1 has shown that domain D1 contains the primary binding site for rhinoviruses as well as the binding site for its natural ligand, lymphocyte function-associated antigen 1 (20–23). Other surface antigens within the immunoglobulin superfamily that are used by viruses as receptors include CD4 for human immunodeficiency virus type 1 (24–27), the poliovirus receptor (28), and the mouse coronavirus receptor (29). In ICAM-1, the poliovirus receptor (30, 31), and in CD4 (32) the primary receptor–virus binding site is domain D1. The structures of the two amino-terminal domains of CD4 have been determined to atomic resolution (33, 34). Truncated proteins corresponding to the two amino-terminal domains of ICAM-1 [tICAM-1(185)] as well as the intact extracellular portion of ICAM-1 [tICAM-1(453) or domains D1–D5] have been expressed in CHO cells (35). The desialated form of tICAM-1(185), which will be referred to hereafter as molecule D1D2, has recently been crystallized (36).

A model of the amino-terminal domain D1 of ICAM-1, based on its homology to known structures of the constant domains of immunoglobulins, was reported by Giranda *et al.* (37). Guided by mutational studies of HRV-14 and ICAM-1, they were able to fit this model into the known canyon structure of HRV-14. We have used cryoelectron microscopy and image-analysis techniques to calculate a three-dimensional reconstruction of the complex of HRV-16 and D1D2 to ≈28-Å resolution. The reconstruction clearly shows that the receptor binds into the canyon of rhinovirus as predicted (1, 8). In addition, we use the known structures of HRV-14 and CD4 and the predicted structure of domain D1 of ICAM-1 to identify atomic interactions.

METHODS AND RESULTS

Structure of the Virus–Receptor Model. Complexes between HRV-16 and ICAM-1 D1D2 were prepared by incubating a solution of HRV-16 at 3.3 mg/ml with a solution of D1D2 at 6.6 mg/ml for ≈16 hr at 34°C. Under these conditions, saturated complexes of HRV-16 with D1D2 can be generated, with ≈60 mol of D1D2 per mol of virus. HRV-14 could also form complexes, although these complexes rapidly broke down to empty capsids (H. Hoover–Litty and J.M.G., unpublished results) and electron micrographs of such specimens revealed severely disrupted particles in a background of protein. HRV-16 complexes with D1D2 or with the complete D1–D5 extracellular-domain fragment were both used in

The publication costs of this article were defrayed in part by page charge payment. This article must therefore be hereby marked "*advertisement*" in accordance with 18 U.S.C. §1734 solely to indicate this fact.

Abbreviations: ICAM-1, intercellular adhesion molecule 1; HRV, human rhinovirus; HRV-14, HRV-16, and HRV-1A, HRV type 14, 16, and 1A, respectively; D1D2, desialated form of truncated ICAM-1-(1–185) that includes domains 1 and 2.

‡Present address: Genetic Therapy Inc., 19 Firstfield Road, Gaithersburg, MD 20878.
§To whom reprint requests should be addressed.

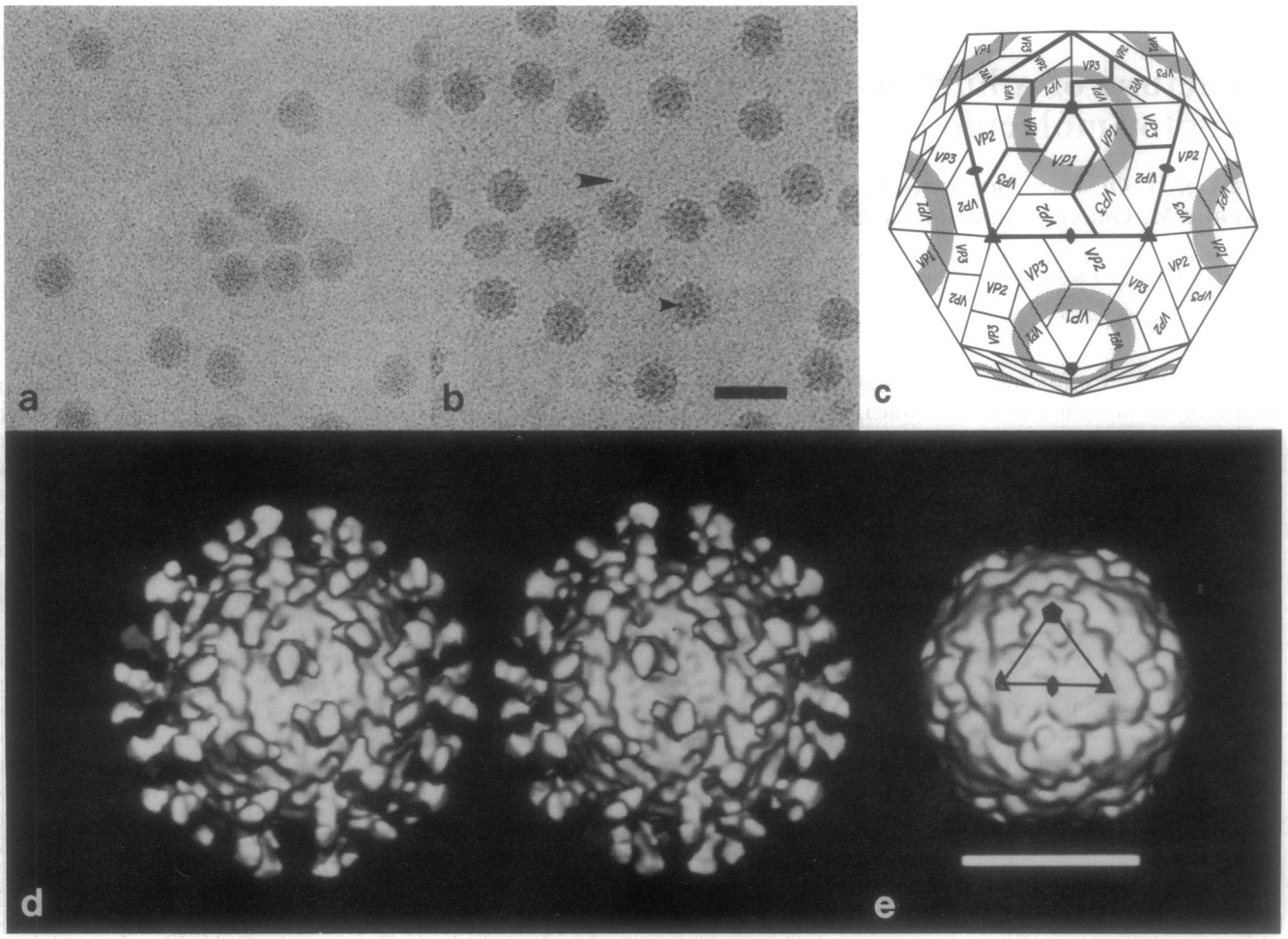

FIG. 1. Cryoelectron microscopy of human rhinovirus (HRV)-16 particles and their complex with D1D2. The microscopy was done essentially as described by Cheng *et al.* (3) with images recorded at a magnification of ×47,500 and with an electron dose of ≈20 electrons per Å^2. (*a*) Native HRV-16. (*b*) HRV-16–D1D2 complex. D1D2 molecules (the two amino-terminal domains of ICAM-1) are seen edge-on at the periphery of the virions (large arrowhead) or end-on in projection (small arrowhead). (*c*) Schematic diagram of HRV showing the icosahedral symmetry, subunit organization, and canyon (shaded). Thick lines encircle five protomers of VP1–VP3. The fourth viral protein, VP4, is inside the capsid. (*d*) Stereoview of reconstruction of the HRV-16–D1D2 complex, viewed along an icosahedral 2-fold axis in approximately the same orientation as in *c*. Sixty D1D2 molecules are bound to symmetry-equivalent positions at the 12 canyon regions on the virion. The reconstruction was modified to correct for defocus and amplitude-contrast effects present in the original micrographs (4). (*e*) Shaded-surface view of HRV-14, computed from the known atomic structure (1), truncated to 20-Å resolution. The triangular outline of one icosahedral asymmetric unit corresponding to that in *c* is indicated. [Bar = 500 Å (*a* and *b*); 200 Å (*d* and *e*).]

the investigation. We present here only the results obtained on the HRV-16–D1D2 complex.

Unstained, vitrified HRV-16 and HRV-16–D1D2 (Fig. 1 *a* and *b*) have very low, inherent contrast, and the recorded micrographs were very noisy because of the required levels of defocus (≈0.8 μm) and irradiation (≈20 electrons per Å^2). The only readily visible details on the complexes (Fig. 1*b*) are the D1D2 molecules that are seen either edge-on at the periphery of the virions or end-on in projection. Forty-four images of the complex were combined to compute a three-dimensional reconstruction (Fig. 1*d*) with an effective resolution of ≈28 Å (38). Although each of the images could be aligned with respect to a consistent choice of enantiomorph, in the absence of additional information there was no way to determine the absolute hand of the reconstruction. However, the asymmetric distribution of density features about the 3- and 5-fold axes in both the reconstruction and the known HRV-14 structure (Fig. 1*e*) was clearly evident and unambiguously established that the reconstruction had been computed with the correct hand. The excellent correspondence between the asymmetric features provided added confirmation that the reconstruction was accurate. Furthermore, the correlation coefficient between the EM and x-ray maps for densities between radii of 125–150 Å was 0.67 for the correct hand versus 0.53 for the opposite hand. The density value of the D1D2 feature in the reconstruction was roughly the same as the density of the virion capsid, thus indicating that the D1D2 molecules nearly saturated the 60 available sites on the virion. The position of the ICAM relative to the icosahedral symmetry axes of the virus is unambiguous. Each D1D2 molecule has an approximate dumbbell shape, consistent with the presence of a two-domain structure.

A difference map between the EM density and the 20-Å-resolution HRV-14 density (Fig. 2) showed that the D1D2 molecule binds to the central portion of the canyon in a manner roughly as predicted by Giranda *et al.* (37), confirming the predictions inherent in the canyon hypothesis (6). This map also showed that the D1D2 molecule has more extensive association with the "southern" than the "northern" (Fig. 3) wall and rim of the canyon. The binding site is near the center of the triangle formed between a 5-fold and two adjacent 3-fold axes (Fig. 3). The ICAM fragment is oriented roughly perpendicular to the viral surface and extends to a radius of ≈205 Å. Its total length is ≈75 Å, as measured in the difference map.

Studies with interspecies chimeras and site-directed mutagenesis of ICAM-1 aimed at identifying the regions neces-

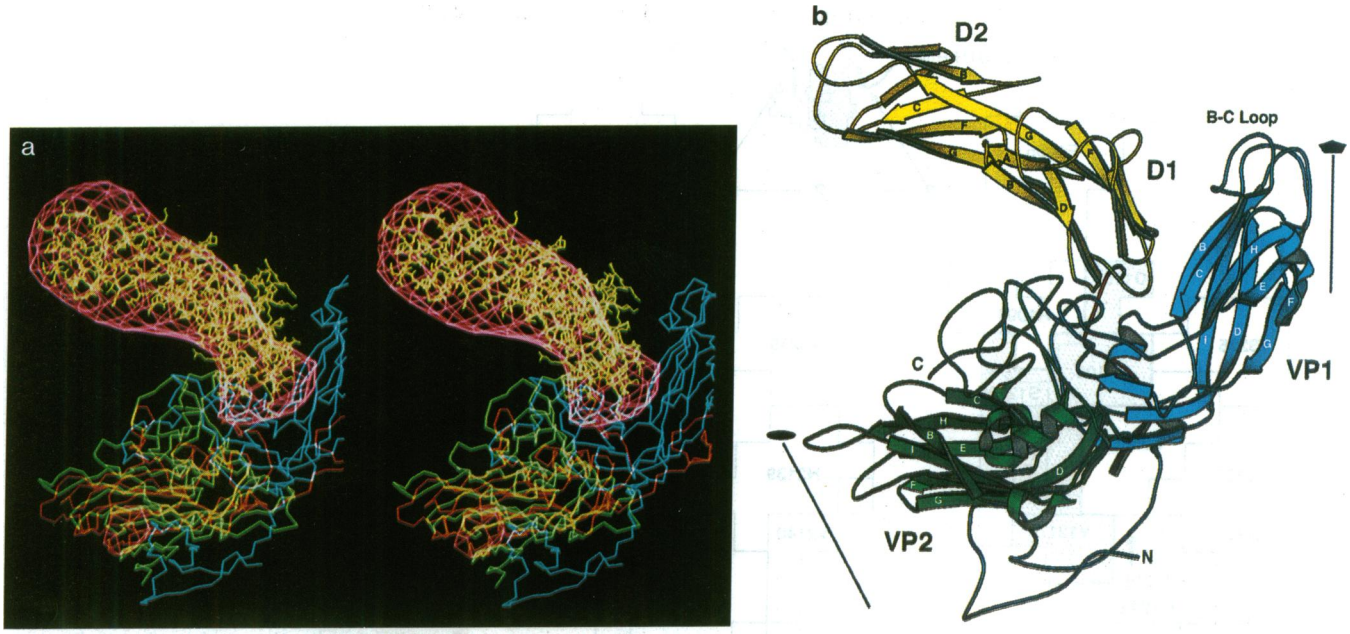

FIG. 2. (*a*) Stereodiagram showing the fit of the CD4 structure into the difference density between the HRV-16–D1D2 reconstruction (Fig. 1*d*) and the x-ray map of HRV-14 (Fig. 1*e*). A radial scale factor was first determined to slightly adjust the EM model to the accurate dimensions of the x-ray model. The difference electron density is shown in scarlet, the CD4 amino-terminal two-domain structure is shown in yellow, and the HRV-14 structure is shown in blue (VP1), green (VP2), and red (VP3). The additional strands $\beta C'$ and $\beta C''$ in D1 of CD4 compared with ICAM-1 lie outside the difference density. (*b*) Diagrammatic drawing (39) of the structure shown in *a*. Secondary-structural elements of the CD4 fragment and of HRV-14 (homologous structures used to represent ICAM-1 and HRV-16, respectively) are identified by the nomenclature in which the first digit signifies the viral protein and the last three digits give the amino acid-sequence number within the protein. The amino and carboxyl termini of VP1 are also marked.

sary for rhinovirus binding indicated that only the first domain is essential and that the residues most involved in virus binding were concentrated on the outside end of domain D1 (21, 22). However, it has proven difficult to produce an active form of domain D1 in solution, domains D1 plus D2 being the minimal soluble virus-binding species (35). The inability to produce domain D1 in isolation and the sequence alignment between ICAM-1 and CD4 suggested that domains D1 and D2 of ICAM-1 are intimately associated through a common, extended β-strand, as is seen in the structure of CD4 (33, 34). Thus, it seemed reasonable to use the known structures of CD4 for fitting the reconstructed density map (Fig. 2), although there was slightly too little density for domain D1 and too much density for D2. A better assessment of the fit of domain D1 to the density was obtained by taking the predicted D1 structure of ICAM-1, including all side chains, and superimposing it onto the fitted C_α backbone of CD4. One major difference is that although domain D1 of CD4 resembles a variable, immunoglobulin-like domain with two extra β-strands, the ICAM-1 prediction is based on a more likely analogy to an immunoglobulin constant domain. This gives domain D1 of ICAM-1 a sleeker appearance, consistent with the observed difference density (Fig. 2*a*). The extra density in D2 [in the region farthest away from the virus (Fig. 2*a*)] compared with domain D2 of CD4 is probably due to the associated carbohydrate groups located in this region.

The atomic structure of HRV-14 closely matched the reconstructed density that was not occupied by the D1D2 fragment. The only exception occurred in the B-C loop of VP1 of HRV-14 (see Fig. 2), which extended ≈3 Å outside the reconstructed density on the northern rim of the canyon. However, this region of the polypeptide chain is a highly variable structure and is the site of one of the two largest conformational differences between HRV-14 and HRV-1A (17). It is also the site of major differences in the structures of homologous poliovirus serotypes 1 and 3 (41).

Mutational Data. The footprint of ICAM on the HRV-14 structure correlates very well with evidence from mutagenesis of the virus (Fig. 3). Colonno *et al.* (9) showed that HRV-14 residues H1220 (the first digit of the residue identification signifies the viral protein, whereas the last three digits give the amino acid-sequence number within the protein), K1103, P1155, and S1223 all affect binding of the virus to cellular membranes. All of these residues are part of the canyon floor and lie centrally within the footprint of the D1D2 molecule-binding site (Fig. 3). Certain antiviral agents to rhino- and enteroviruses (42) inhibit uncoating and attachment. These agents bind to a pocket beneath the canyon and, in HRV-14, significantly alter the structure of the canyon floor (40). These conformational changes inhibit viral attachment (10, 43) and are now shown to be exactly at the site of ICAM-1 attachment (Fig. 3).

The parts of the predicted ICAM-1 structure that contact HRV-14 are the amino-terminal four residues and loops B-C (residues 24–26), D-E (residues 45–49), and F-G (residues 71 and 72; see Fig. 2 for nomenclature). Staunton *et al.* (21), McClelland *et al.* (22), and Register *et al.* (44) have examined the effects of a number of site-directed mutations and mouse–human substitutions in domain D1 of ICAM-1 on rhinovirus binding. On the basis of these reports seven regions in D1, corresponding roughly to the amino terminus (residues 1 and 2), loop B-C (residues 26–29), strand D (residues 40 and 43), loop D-E (residues 46–48), strand F (residue 67), loop F-G (residues 70–72), and the G strand (residues 75–77) have been implicated in virus binding. There is correspondence to, or significant overlap between, the four regions of ICAM-1 seen here to be in contact with rhinovirus and four of the seven regions identified by site-directed mutagenesis. Thus, there appears to be reasonable agreement between the mutational studies of ICAM-1 and the observed virus–receptor contacts of the complex.

DISCUSSION

The structure of a complex of simian rotavirus with a neutralizing-antibody Fab fragment was studied by cryoelec-

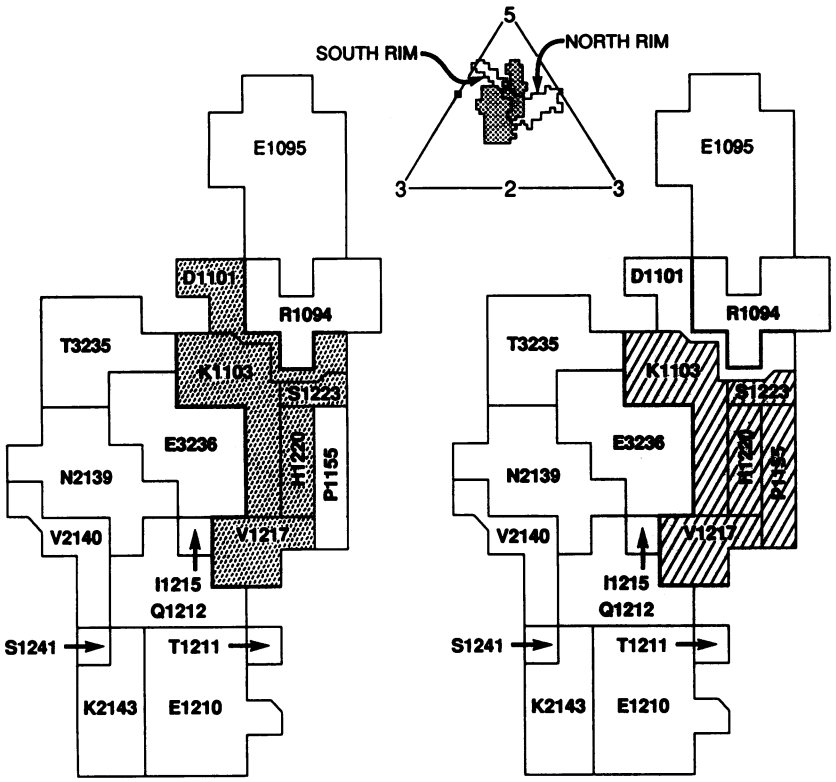

FIG. 3. (*Top*) View of the icosahedral asymmetric unit bounded by adjacent 5- and 3-fold axes, outlining residues on the viral surface. The limits of the canyon are shown, arbitrarily demarcated by a 138-Å radial distance from the viral center (5), and the ICAM-1 footprint (stippled). Improved resolution of the electron density could only marginally alter the HRV residues at the virus–receptor interface. (*Left* and *Right*) Enlarged view of the residues in the ICAM-1 footprint showing the residues (hatched areas) that, when mutated, affect viral attachment (*Right*) (9), and the residues (stippled areas) altered in structure by the binding of antiviral compounds that inhibit attachment and uncoating (*Left*) (40).

tron microscopy in a manner similar to that reported here (45); however, neither the structure of the virus nor the antibody was known in atomic detail. Recently, the structure of a complex of cowpea mosaic virus and a bound monoclonal antibody Fab fragment was determined with EM (46). In that case, an atomic resolution structure of cowpea mosaic virus was known, permitting determination of the antibody footprint on the viral surface. Even more recently, the structure of a neutralizing-antibody Fab fragment, complexed with HRV-14, has been determined (51), which suggests the mode of bivalent attachment required for neutralization. Here these cryoelectron microscopy techniques are applied to a virus–receptor complex.

Weis *et al.* (12) and Sauter *et al.* (47) have explored the interaction of a carbohydrate moiety on the surface of erythrocytes to which influenza virus can attach. We describe here the structure of a virus–receptor complex in which the receptor is a membrane-bound glycoprotein molecule that is used by a virus for recognition of a specific host tissue for attachment and subsequent entry. This receptor molecule belongs to the immunoglobulin superfamily, a class of molecules frequently used on cell surfaces for the recognition of other molecules (or recognized by viruses) that are subsequently transferred across the membrane. Although the structure of CD4 is known (33, 34), the structure of the human immunodeficiency virus–CD4 complex is not. Mutational studies suggest that the structure recognized by human immunodeficiency virus is a ridge made up of β-strands C″ and D.

Because the general nature of the complex described here had been predicted on the basis of the strategy used by HRV to hide its receptor attachment site, perhaps many other viruses use a similar strategy. Poliovirus is clearly homologous to HRV, and both poliovirus (28) and the major rhinovirus group use an immunoglobulin-like molecule as receptor. Thus, it would be expected that the poliovirus receptor binds into the poliovirus canyon in a manner similar to that of the complex formed for rhinoviruses (31). The structure of a mouse-adapted chimera of human poliovirus 2 has been determined (48). The major structural change occurs in the chimera in the B-C loop, not in the canyon floor. In this instance, therefore, the B-C loop might modulate the virus–receptor interaction.

The determination of residues involved in receptor binding should make it possible to ascertain the origin of specificity of the major rhinovirus serotypes for ICAM-1. Comparison of the amino acid sequences of six rhinoviruses belonging to the major receptor group against four of the minor receptor group did not reveal any clear differentiation. Specificity for the minor receptor may reside in the tendency of the virus to bind a cellular fatty acid tightly (15, 41) (K. H. Kim *et al.*, unpublished work) and thus alter the shape of the canyon floor, rather than the identity of the canyon surface residues themselves. Nevertheless, knowledge of the virus–receptor interaction will illuminate various strategies currently being developed to interfere with early stages of rhinoviral and other viral infections (35, 49, 50).

We are grateful for the many helpful discussions with Roland Rueckert (University of Wisconsin) and Mark McKinlay, Frank Dutko, Guy Diana, and Dan Pevear (Sterling–Winthrop Pharmaceuticals, Research Division). We are also grateful to Marcia Kremer, Carla Forte, and Cindy Music for technical assistance. We thank Wayne Hendrickson and Steve Harrison for sharing coordinate information and Helene Prongay and Sharon Wilder for help in preparing this manuscript. The work was supported by National Institutes of Health grants to M.G.R. and to T.S.B., a National Science Foundation grant to T.S.B., and a Lucille P. Markey Foundation Award. P.R.K. is the recipient of a Jane Coffin Childs Postdoctoral Fellowship.

1. Rossmann, M. G., Arnold, E., Erickson, J. W., Frankenberger, E. A., Griffith, J. P., Hecht, H. J., Johnson, J. E., Kamer, G., Luo, M., Mosser, A. G., Rueckert, R. R., Sherry, B. & Vriend, G. (1985) *Nature (London)* **317**, 145–153.
2. Hogle, J. M., Chow, M. & Filman, D. J. (1985) *Science* **229**, 1358–1365.
3. Cheng, R. H., Olson, N. H. & Baker, T. S. (1992) *Virology* **186**, 655–668.
4. Cheng, R. H. (1992) in *Proceedings of the 50th Annual Meeting of the Electron Microscope Society of America*, eds. Bailey,

G. W., Bentley, J. & Small, J. A. (San Francisco Press, San Francisco), pp. 996–997.
5. Rossmann, M. G. & Palmenberg, A. C. (1988) *Virology* **164**, 373–382.
6. Sherry, B. & Rueckert, R. (1985) *J. Virol.* **53**, 137–143.
7. Sherry, B., Mosser, A. G., Colonno, R. J. & Rueckert, R. R. (1986) *J. Virol.* **57**, 246–257.
8. Rossmann, M. G. (1989) *J. Biol. Chem.* **263**, 14587–14590.
9. Colonno, R. J., Condra, J. H., Mizutani, S., Callahan, P. L., Davies, M. E. & Murcko, M. A. (1988) *Proc. Natl. Acad. Sci. USA* **85**, 5449–5453.
10. Pevear, D. C., Fancher, M. J., Felock, P. J., Rossmann, M. G., Miller, M. S., Diana, G., Treasurywala, A. M., McKinlay, M. A. & Dutko, F. J. (1989) *J. Virol.* **63**, 2002–2007.
11. Kim, S., Boege, U., Krishnaswamy, S., Minor, I., Smith, T. J., Luo, M., Scraba, D. G. & Rossmann, M. G. (1990) *Virology* **175**, 176–190.
12. Weis, W., Brown, J. H., Cusack, S., Paulson, J. C., Skehel, J. J. & Wiley, D. C. (1988) *Nature (London)* **333**, 426–431.
13. Abraham, G. & Colonno, R. J. (1984) *J. Virol.* **51**, 340–345.
14. Uncapher, C. R., DeWitt, C. M. & Colonno, R. J. (1991) *Virology* **180**, 814–817.
15. Kim, S., Smith, T. J., Chapman, M. S., Rossmann, M. G., Pevear, D. C., Dutko, F. J., Felock, P. J., Diana, G. D. & McKinlay, M. A. (1989) *J. Mol. Biol.* **210**, 91–111.
16. Tomassini, J. E., Maxson, T. R. & Colonno, R. J. (1989) *J. Biol. Chem.* **264**, 1656–1662.
17. Greve, J. M., Davis, G., Meyer, A. M., Forte, C. P., Yost, S. C., Marlor, C. W., Kamarck, M. E. & McClelland, A. (1989) *Cell* **56**, 839–847.
18. Staunton, D. E., Merluzzi, V. J., Rothlein, R., Barton, R., Marlin, S. D. & Springer, T. A. (1989) *Cell* **56**, 849–853.
19. Simmons, D., Makgoba, M. W. & Seed, B. (1988) *Nature (London)* **331**, 624–627.
20. Staunton, D. E., Marlin, S. D., Stratowa, C., Dustin, M. L. & Springer, T. A. (1988) *Cell* **52**, 925–933.
21. Staunton, D. E., Dustin, M. L., Erickson, H. P. & Springer, T. A. (1990) *Cell* **61**, 243–254.
22. McClelland, A., deBear, J., Yost, S. C., Meyer, A. M., Marlor, C. W. & Greve, J. M. (1991) *Proc. Natl. Acad. Sci. USA* **88**, 7993–7997.
23. Lineberger, D. W., Graham, D. J., Tomassini, J. E. & Colonno, R. J. (1990) *J. Virol.* **64**, 2582–2587.
24. Robey, E. & Axel, R. (1990) *Cell* **60**, 697–700.
25. Dalgleish, A. G., Beverley, P. C. L., Clapham, P. R., Crawford, D. H., Greaves, M. F. & Weiss, R. A. (1984) *Nature (London)* **312**, 763–767.
26. Klatzmann, D., Champagne, E., Chamaret, S., Gruest, J., Guetard, D., Hercend, T., Gluckman, J. C. & Montagnier, L. (1984) *Nature (London)* **312**, 767–768.
27. Maddon, P. J., Dalgleish, A. G., McDougal, J. S., Clapham, P. R., Weiss, R. A. & Axel, R. (1986) *Cell* **47**, 333–348.
28. Mendelsohn, C. L., Wimmer, E. & Racaniello, V. R. (1989) *Cell* **56**, 855–865.
29. Williams, R. K., Jiang, G.-S. & Holmes, K. V. (1991) *Proc. Natl. Acad. Sci. USA* **88**, 5533–5536.
30. Koike, S., Ise, I. & Nomoto, A. (1991) *Proc. Natl. Acad. Sci. USA* **88**, 4104–4108.
31. Freistadt, M. S. & Racaniello, V. R. (1991) *J. Virol.* **65**, 3873–3876.
32. Arthos, J., Deen, K. C., Chaikin, M. A., Fornwald, J. A., Sathe, G., Sattentau, Q. J., Clapham, P. R., Weiss, R. A., McDougal, J. S., Pietropaolo, C., Axel, R., Truneh, A., Maddon, P. J. & Sweet, R. W. (1989) *Cell* **57**, 469–481.
33. Wang, J., Yan, Y., Garrett, T. P. J., Liu, J., Rodgers, D. W., Garlick, R. L., Tarr, G. E., Husain, Y., Reinherz, E. L. & Harrison, S. C. (1990) *Nature (London)* **348**, 411–418.
34. Ryu, S. E., Kwong, P. D., Truneh, A., Porter, T. G., Arthos, J., Rosenberg, M., Dai, X., Xuong, N., Axel, R., Sweet, R. W. & Hendrickson, W. A. (1990) *Nature (London)* **348**, 419–426.
35. Greve, J. M., Forte, C. P., Marlor, C. W., Meyer, A. M., Hoover-Litty, H., Wunderlich, D. & McClelland, A. (1991) *J. Virol.* **65**, 6015–6023.
36. Kolatkar, P. R., Oliveira, M. A., Rossmann, M. G., Robbins, A. H., Katti, S. K., Hoover-Litty, H., Forte, C., Greve, J. M., McClelland, A. & Olson, N. H. (1992) *J. Mol. Biol.* **225**, 1127–1130.
37. Giranda, V. L., Chapman, M. S. & Rossmann, M. G. (1990) *Proteins* **7**, 227–233.
38. Baker, T. S., Newcomb, W. W., Olson, N. H., Cowsert, L. M., Olson, C. & Brown, J. C. (1991) *Biophys. J.* **60**, 1445–1456.
39. Kraulis, P. J. (1992) *J. Appl. Crystallogr.* **24**, 946–950.
40. Smith, T. J., Kremer, M. J., Luo, M., Vriend, G., Arnold, E., Kamer, G., Rossmann, M. G., McKinlay, M. A., Diana, G. D. & Otto, M. J. (1986) *Science* **233**, 1286–1293.
41. Filman, D. J., Syed, R., Chow, M., Macadam, A. J., Minor, P. D. & Hogle, J. M. (1989) *EMBO J.* **8**, 1567–1579.
42. Diana, G. D., McKinlay, M. A., Otto, M. J., Akullian, V. & Oglesby, C. (1985) *J. Med. Chem.* **28**, 1906–1910.
43. Heinz, B. A., Rueckert, R. R., Shepard, D. A., Dutko, F. J., McKinlay, M. A., Fancher, M., Rossmann, M. G., Badger, J. & Smith, T. J. (1989) *J. Virol.* **63**, 2476–2485.
44. Register, R. B., Uncapher, C. R., Naylor, A. M., Lineberger, D. W. & Colonno, R. J. (1991) *J. Virol.* **65**, 6589–6596.
45. Prasad, B. V. V., Burns, J. W., Marietta, E., Estes, M. K. & Chiu, W. (1990) *Nature (London)* **343**, 476–479.
46. Wang, G., Porta, C., Chen, Z., Baker, T. S. & Johnson, J. E. (1992) *Nature (London)* **355**, 275–278.
47. Sauter, N. K., Glick, G. D., Crowther, R. L., Park, S. J., Eisen, M. B., Skehel, J. J., Knowles, J. R. & Wiley, D. C. (1992) *Proc. Natl. Acad. Sci. USA* **89**, 324–328.
48. Yeates, T. O., Jacobson, D. H., Margin, A., Wychowski, C., Girard, M., Filman, D. J. & Hogle, J. M. (1991) *EMBO J.* **10**, 2331–2341.
49. McKinlay, M. A., Pevear, D. C. & Rossmann, M. G. (1992) *Annu. Rev. Microbiol.* **46**, 635–654.
50. Marlin, S. D., Staunton, D. E., Springer, T. A., Stratowa, C., Sommergruber, W. & Merluzzi, V. J. (1990) *Nature (London)* **344**, 70–72.
51. Smith, T. J., Olson, N. H., Cheng, R. H., Chase, E., Lee, W.-M., Leippe, D., Mosser, A., Rueckert, R. R. & Baker, T. S. (1993) *J. Virol.*, in press.